UAV Path Planning for Maximum-Information Sensing in Spatiotemporal Data Acquisition

By:
Andreas Nordby Vibeto
andreanv@stud.ntnu.no

Supervisor: **Tor Arne Johansen**

Co-supervisor: Joo F. Fortuna

May, 2017

Contents

Chapter 1

Introduction

Unmanned Aerial Vehcles (UAV) are today widely used in ground observation, and by equipping them with different sensors they can be used in different situations. While the use of UAV eases many cases of ground obsercation, there are some difficulties related to the attitude of the aircraft. When the sensor is attached directly to the aircraft the sensor will be coupled with the UAVs states, so that any change in the UAV states will cause a change in what is actually observed by the sensor. An illustration of this is shown in figure 1.1.

A common solution to decouple the sensor from the UAV states is to attach the sensor to a gimbal which will countaract most of the movements of the UAV. While this is a good solution for decoupling, it raises some new issues regarding its weight and size. As one of the benefits of UAVs is their small size the gimbal can quickly be too big and heavy for the UAV, and it may give less effective aerodynamics. This may again lead to increased fuel consumption for the UAV.

This paper will investigate methods to reduce image errors caused by the UAVs attitude, while also avoiding the extra costs associated with a gimbal. This will be accomplished by optimizing a pre-defined curved path that is to be observed with a model of the UAV. The control method will be developed with a hyperspectral pushbroom camera that is fixed to the UAV in mind.

1.1 Related Work

The most common method to decouple the UAV attitude states from the sensor today is to equip the aircraft with a gimbal, which allows ”NORMAL” UAV operation without losing track of the features that is to be observed. However, gimbals have limited range and if the UAV angles are to big, the features may be lost from the sensor field of view (FOV). One solution to this problem is to use optimization [1]. Another solution that

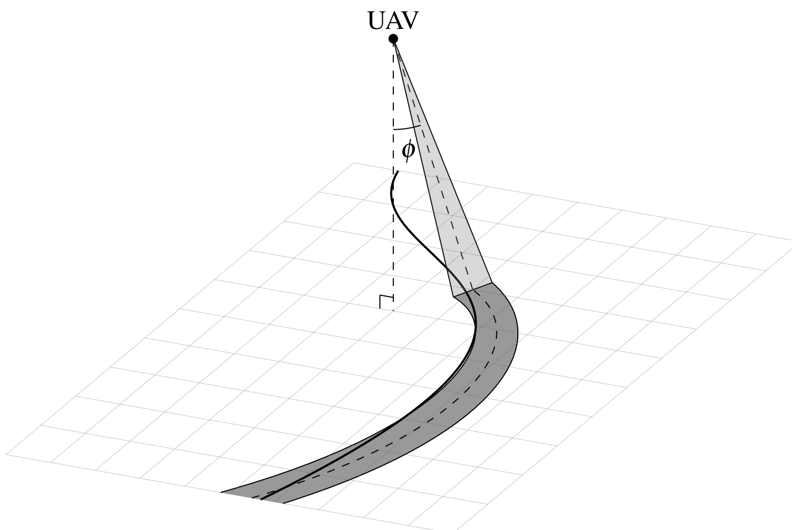

Figure 1.1: An illustration showing a UAV that uses a camera fixed to its body to observe a ground path, and how the position of the camera footprint relates to the UAV attitude.

uses optimization without the use of gimbal is to put constraints on the the UAVs roll angle and altitude [2].

A simpler solution to avoid lateral movements of the FOV is to change the UAV course wby using the rudder instead of the ailerons. The rudder deflection creates a yawing moment [3] which causes the aircraft to change course. This type of controller is referred to both as a Rudder Augmented Trajectory Correction (RATC) controller [3] and a skid-to-turn (STT) controller [4]. Results show that the performance of these controllers are comparable to conventional controllers using roll to change course, and that errors in the images is greatly reduced [3] [4] [5].

While the controllers offer a solution to the control problem that reduces the errors in the images, they do not ensure that the ground path that is to be observed will always stay inside the sensors FOV. Optimization is a commonly used method for ensuring that the application succeeds at some ”outside” goal, and can be used to e.g. minimize the risk of being identified by radars [6] or plan a path that ensures that a slung load attached to a helicopter do not collide with obstacles [7]. The use of optimization to minimize the error of the sensor footprint for a fixed camera has been done by Jackson [8], by using on-board motion planning.

Jackson presents a path planner that aims to minimize the error between the target on the ground, and the footprint of a camera fixed to a UAV. To achieve this a Nonlinear Model Predictive Controller (NMPC) based on a kinodynamic (an explenation of this would be nice) model of the aircraft is created. The NMPC is compared to a PID and a sliding-mode controller that seek to follow the same path. Simulations of the three controllers show that while the PID controller had much bigger crosstrack errors than the other two, the NMPC and the sliding-mode controller had similar performance. However, the simulations proved that the NMPC controller was able to find a near optimal solution with the performance characteristics of a real-time application.

1.2 Hyperspectral Imaging

The control method developed in this paper will be developed with the use of a fixed hyperspectral, pushbroom sensor in mind. A hyperspectral sensor/camera makes it possible to accurately detect types of material from the UAV by sensing the wavelength of the received light.

1.2.1 Description

Hyperspectral imaging uses basics from spectroscopy to create images, which means that the basis for the images is the emitted or reflected light from materials [9]. The amount of light that is reflected by a material at different wavelengths is determined by several factors, and this makes it possible to distinguish different materials from each other. The reflected light is passed through a grate or a prism that splits the light into different wavelength bands, so that it can be measured by a spectrometer.

When using a hyperspectral camera for ground observation from a UAV, it is very likely that one pixel of the camera covers more than one type of material on the ground. This means that the observed wavelengths will be influenced by more than one type of material. This is called a composite or mixed spectrum [9], and the spectra of the different materials are combined additively. The combined spectra can be split into the different spectra that it is build up of by noise removal and other statistical methods which will not be covered here.

1.2.2 UAV Ground Observation

Hyperspectral imaging is already being used for ground observation from UAVs. Its ability to distinguish materials based on spectral properties means that it can be used to retrieve information that normal cameras are not able to. For example in agriculture it can be used to map damage to trees caused by bark beetles [10], or it can be used to measure environmental properties, for example chlorophyl fluorescense, on leaf-level in a citrus orchard [11].

Systems for ground observation with hyperspectral cameras can be very complex, which often leads to heavy systems. In [12], a lightweight hyperspectral mapping system was created for the use with octocopters. The purpose of the system is to map agricultural areas using a spectrometer and a photogrammetric camera, and the final ”ready-to-fly” weight of the system is 2.0 kg. The resolution of the final images made it possible to gather information on a single-plant basis, and the georeferencing accuracy was off by only a few pixels.

The tests were performed at a low altitude, maximum 120 m. While this was mainly because of local regulations, it also gave a benefit as there was less atmosphere disturbance in the measurements. The UAVs orientation data combined with surface models was used when recovering the positional data in the images. However, they found that externally produced surface models was not accurate enough as they do not take vegetation into consideration. For this reason they supplemented the existing surface models with information gathered during flight.

1.3 Thesis Outline

Chapter 2

Kinematics

What is captured by the camera, the camera footprint, when the camera is fixed to the aircraft body is dependent of the position and the attitude angles of the aircraft. In this section a model for calculating the camera footprint on the ground assuming flat earth will be presented, as well as the necessary UAV states for this thesis.

2.1 Linear UAV Model

2.2 UAV States

The position of the UAV will be given using the North East Down (NED) coordinate frame, denoted $\{n\}$:

$$\mathbf{p}_{b/n}^{n} = \begin{bmatrix} N \\ E \\ D \end{bmatrix} = \begin{bmatrix} x_n \\ y_n \\ z_n \end{bmatrix}, \tag{2.1}$$

with the corresponding velocities

$$\mathbf{V}_{g}^{b} = \begin{bmatrix} u \\ v \\ w \end{bmatrix}. \tag{2.2}$$

The attitude of the UAV will be given as Euler-angles:

$$\boldsymbol{\Theta}_{nb} = \begin{bmatrix} \phi \\ \theta \\ \psi \end{bmatrix} \tag{2.3}$$

with corresponding angular velocities:

$$\dot{\mathbf{\Theta}}_{nb} = \begin{bmatrix} p \\ q \\ r \end{bmatrix}. \tag{2.4}$$

2.3 Wind and Airspeed

Wind will be introduced to the vehicle in order to test how the system withstands disturbances. Since the camera footprint is dependent only on the attitude angles of the aircraft and not the course of the aircraft, the wind will only affect the navigation of the UAV. Wind speed is given in the $\{n\}$ frame as [13]

$$\mathbf{V}_w^n = \begin{bmatrix} w_n \\ w_e \\ w_d \end{bmatrix}, \tag{2.5}$$

and the air speed $\mathbf{V}_a$ of the aircraft is given by the wind speed $\mathbf{V}_w$ and ground speed $\mathbf{V}_g$ as

$$\begin{gathered} \mathbf{V}_a = \mathbf{V}_g - \mathbf{V}_w \\ \begin{bmatrix} u_r \\ v_r \\ w_r \end{bmatrix} = \begin{bmatrix} u \\ v \\ w \end{bmatrix} - \mathbf{R}_n^b \begin{bmatrix} w_n \\ w_e \\ w_d \end{bmatrix} \end{gathered} \tag{2.6}$$

where $\mathbf{R}_n^b$ is the rotation matrix between the NED frame $\{n\}$ and the body frame $\{b\}$.

When in the presence of wind, the heading of the UAV isn't necessarily the direction that the UAV is moving. Wind will introduce a crab angle χ_c that together with the heading ψ gives the course angle χ:

$$\chi = \psi + \chi_c. \tag{2.7}$$

2.4 Camera Footprint

The camera footprint is coupled with all of the three angles given in $\mathbf{\Theta}$. The position of the camera footprint will be calculated using forward kinematics, and the situation is shown in figure 2.1.

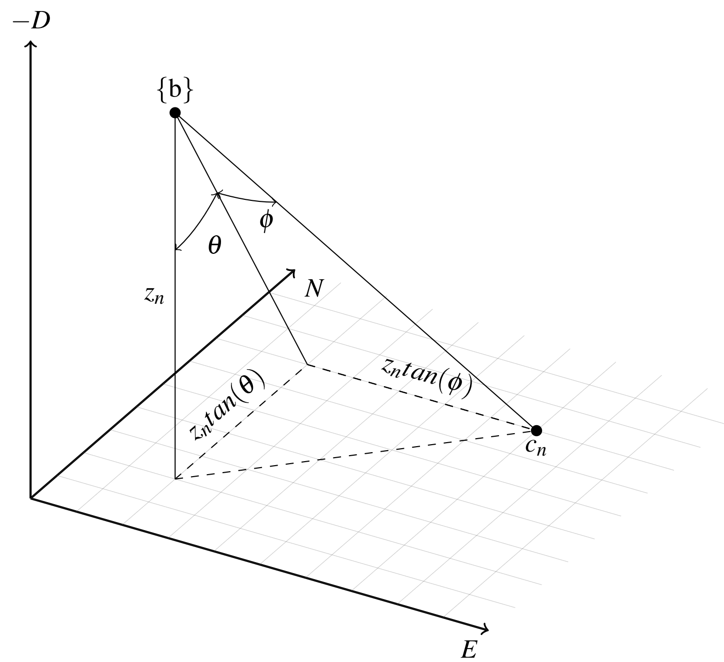

Figure 2.1: Illustration of how the aircraft attitude influence the camera position.

2.4.1 Centre Position

The attitude of the UAV is given in the body frame $\{b\}$ and the height z_n is given in the NED frame $\{n\}$, and the model assumes flat earth. The position of the footprint centre point $\mathbf{c}_b^b$ in the body frame $\{b\}$ is expressed as the geometric (???) distance from the UAV position to the footprint centre point:

$$\mathbf{c}_b^b = \begin{bmatrix} c_{x/b}^b \\ c_{y/b}^b \end{bmatrix} = \begin{bmatrix} z_n tan(\theta) \\ z_n tan(\phi) \end{bmatrix}. \tag{2.8}$$

The coordinates of the camera position in $\{n\}$ can be found by rotating the point $\mathbf{c}_b^b$ with respect to the aircraft heading ψ, and by translating the rotated point to the aircrafts position in the $\{n\}$ frame. The rotation matrix for rotating with respect to the heading is given as

$$\mathbf{R}_{z,\psi} = \begin{bmatrix} cos(\psi) & -sin(\psi) \\ sin(\psi) & cos(\psi) \end{bmatrix}. \tag{2.9}$$

The final expression for the camera footprint centre position $\mathbf{c}^n$ in the $\{n\}$ frame then becomes:

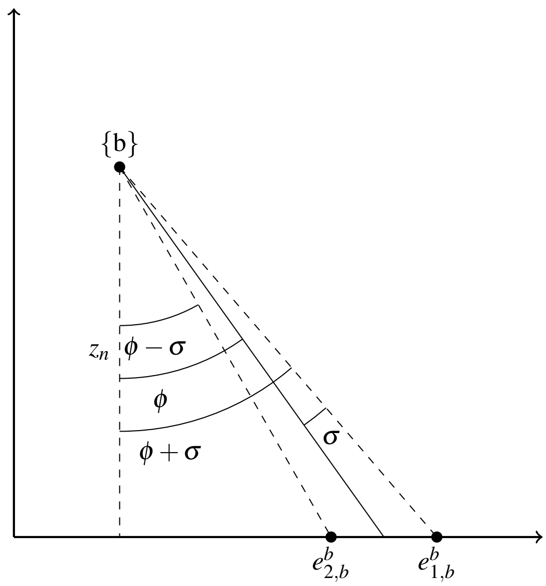

Figure 2.2: Illustration of how the field of view for a pushbroom sensor is calculated.

$$\begin{aligned}\mathbf{c}^n &= \mathbf{p} + \mathbf{R}_{z,\psi}\mathbf{c}^b_b \\ &= \begin{bmatrix} x_n \\ y_n \end{bmatrix} + \mathbf{R}_{z,\psi}\begin{bmatrix} x^b_{x/b} \\ c^b_{y/b} \end{bmatrix}\end{aligned} \tag{2.10}$$

2.4.2 Edge Points

A hyperspectral pushbroom sensor captures images in a line, and the centre point of the camera footprint does not express the entire area that is captured by the sensor. The edge points of the camera footprint are calculated with respect to the sensor's field of view, as shown in figure 2.2. These points **e** can be found by altering 2.8:

$$\mathbf{e}^b_{1,b} = \begin{bmatrix} z_n tan(\theta) \\ z_n tan(\phi + \sigma) \end{bmatrix}, \ \mathbf{e}^b_{2,b} = \begin{bmatrix} z_n tan(\theta) \\ z_n tan(\phi - \sigma) \end{bmatrix}. \tag{2.11}$$

The steps for writing the edge points **e** in the $\{n\}$ is similar as in equation 2.10:

$$\mathbf{e}^n = \mathbf{p} + \mathbf{R}_{z,\psi}\mathbf{e}^b_b. \tag{2.12}$$

Chapter 3

Model Predictive Control

Model Predictive Control (MPC) is a term used to describe control methods that uses knowledge about the process to calculate the future control inputs to the system in order to follow a reference trajectory [14]. In this chapter the equations for an *offline intervalwise MPC* that seeks to minimize the distance between the camera centre point and the ground path that is to be observed will be given. A linear state space-model for the UAV will be used to predict the future states and control inputs.

3.1 MPC Method

The MPC strategy can be broken down into three tasks [14]:

1. Predict the future outputs of the process for the given prediction horizon using past inputs to the process and the past measured states of the process, and by using the future control signals.
2. Optimize an objective function in order to determine the future control signals that follows a given reference trajectory as closely as possible.
3. Apply the optimal control signals to the process, and measure the resulting output so that it may be used to calculate the next prediction horizon in the first task.

In short MPC problems are made up of three elements [14]: Prediction model, objective function and the control law. The prediction model represents the model of the process that is to be controlled, and will in this case consist of the differential equations for the states of the UAV. The objective function is the function that is to be minimized by the optimization algorithm, in this case this will be the distance from the camera centre point to the desired ground path together with some of the UAV states that will give a stable flight. The objective function represents the reference trajectory that the UAV is to follow. The control law introduces constraints on the problem, reducing the number of feasible solutions. These constraints can be put on either the states or the control inputs for the UAV.

A common mathematical formulation of the three elements that make up the optimization problem is shown in 3.1 [15]. $f(x)$ represents the objective function that is subject to equality and inequality constraints respectively. The equality constraints are used to represent the UAV model, while the inequality constraints represent the constraints used for the control law. A MPC differ from other optimization problems mostly in the objective function, which will be described in detail chapter 3.3.

$$\begin{aligned} \min_{x \in R^n} \quad & f(x) \\ \text{s.t} \quad & c_i(x) = 0, i \in \varepsilon, \\ & c_i(x) \geq 0, i \in I. \end{aligned} \tag{3.1}$$

3.2 Offline Intervalwise MPC

The control problem in this thesis will be solved by using an offline intervalwise MPC to generate an optimal path that will reduce the image error when using a fixed camera to survey a ground track. The generated path is intended to be tracked by the autopilot on the actual UAV that will perform the survey, with th eintention of optimally surveying the ground path.

3.2.1 Offline MPC

An *offline MPC* means that the initial state of the MPC is not a measurement of the UAV states, but rather the result of a simulation of the UAV. This means that the result from the prediction model used in the MPC will act as the physical system, and the outputs of the model will be fed back as inputs to the MPC for every iteration. The equations of the offline MPC are the same as the ones for the online version.

Rawlings & Mayne [16] refers to this kind of problem as a *deterministic problem* since there is no uncertainty in the system. A feedback loop in this kind of system is also not needed in principle, since it does not present any new information. They also state that an MPC action for a deterministic system is the same as the action from a *receding horizon control law* (RHC), which is another kind of predictive control.

3.2.2 Intervalwise MPC

Altough the feedback is not needed to give new information, it eases the computational load of the control problem as optimizing the path over a long time horizon leads to a very complicated problem. For this reason a *intervalwise MPC* will be used. The term intervalwise has been introduced by Kwon & Han [17] to describe a type of receding horizon controller that implements the same strategy.

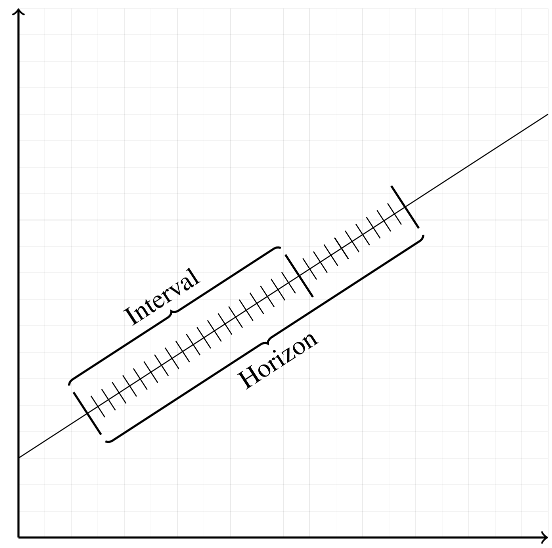

Figure 3.1: The figure shows how the path is divided into sections and horizons when using the intervalwise MPC.

Commonly a MPC is used to optimize the model over a given *horizon*, where the initial states are given. After the optimization has finished the first timestep of the optimization is returned and applied to the system, before a measurement of the system is performed. The new measurements are given as initial states for the next horizon, and so on.

The principle is the same for an intervalwise MPC. However, instead of only returning the first timestep an *interval* of timesteps are returned, and the last timestep of the interval is used as intial states for the next optimization horizon. This way the number of MPC iterations is reduced, and the increased complexity by having long optimization horizons is avoided. Figure 3.1 shows how timesteps, intervals and horizons relate to each other.

3.3 Objective Function

The main objective of the MPC developed in this thesis is to minimize the cross track error between the centre point of the camera footpring and the ground path that is to be observed. This, together with other objectives, will be defined in the objective function of the optimization problem. In this section a way of formulating the objective function, least-squares, will be described, and how it can expressed to function as a MPC.

3.3.1 Least-Squares Problem

In many applications the objective function is formulated as a least-square (LSQ) problem. LSQ is a form of regression where the distance from a certain point to a known model is measured [source]. In this case the known model is the reference signals and the distance between the current states and the reference signal is calculated by the LSQ. The general mathematical formulation for LSQ is [15]:

$$f(x) = \frac{1}{2}\sum_{j=1}^{m} r_j^2(x). \tag{3.2}$$

In equation 3.2 r_j is called the residual function, the distance between the point and the model. In relation to the MPC, the residual function is what the MPC seeks to minimize. The residual function is minimized by finding the parameters x that minmize the residual function r.

3.3.2 MPC Objective Function

The objective function is where the goal of the optimization is expressed, together with the optimization horizon of the problem. Typical goals of the optimization is to follow a predefined trajectory or reference signal while reducing the control inputs used. This can be expressed as follows [14]:

$$J(N_1, N_2, N_3) = \sum_{j=N_1}^{N_2} \delta(j)[\hat{y}(t+j|t) - w(t+j)]^2 + \sum_{j=1}^{N_u} \lambda(j)[\Delta u(t+j-1)]^2. \tag{3.3}$$

The first term of equation 3.3 represents the costs from the states of the model, and the second term represents the cost of the control effort. In the first term $\hat{y}$ is the value of the prediction model, which is compared to the desired trajectory w. In the second term the changes in control Δu is expressed. The changes in control is used instead of the value of the control signal itself, since the steady state of the control signal may not be zero. δ and λ are weighting variables which offers a way of tuning the MPC. The three different N coefficients defines the horizon over which the states and the control effort should be optimized. The optimization horizon for states and control effort can be different, but they will stay the same for this problem.

3.4 Problem Definition

$$\begin{array}{lrcl} \min\limits_{\mathbf{z}} & \mathbf{J}_k = \frac{1}{2}\sum_{i=k}^{k+L}[\mathbf{h}(\mathbf{z}_i)^\intercal \mathbf{Q}\mathbf{h}(\mathbf{z}_i)] + \frac{1}{2}\sum_{i=k}^{k=L}[\mathbf{u}_i^\intercal \mathbf{R}\mathbf{u}_i] & & \\ \text{s.t} & \mathbf{x}^{low} \leq & \mathbf{x}_i & \leq \mathbf{x}^{high} \\ & \mathbf{u}^{low} \leq & \mathbf{u}_i & \leq \mathbf{u}^{high} \\ & \dot{\mathbf{x}} & = & f(\mathbf{x}, \mathbf{u}) \end{array} \tag{3.4}$$

The equations for the full optimization problem is shown in equation 3.4. The objective function uses the same setup as shown in equation 3.3, but on matrix form. Each of the three components of the problem definition will be described in detail in the following sections.

3.4.1 Objective Function

$$\mathbf{J}_k = \frac{1}{2}\sum_{i=k}^{k+L}[\mathbf{h}(\mathbf{z}_i)^\intercal \mathbf{Q}\mathbf{h}(\mathbf{z}_i)] + \frac{1}{2}\sum_{i=k}^{k=L}[\mathbf{u}_i^\intercal \mathbf{R}\mathbf{u}_i] \tag{3.5}$$

The first term of the objective function calculates the distance between the UAV states and the reference trajectory. The vector $\mathbf{z}$ is the optimization vector that contains the UAV states that will be included in the optimization problem and $\mathbf{Q}$ is the weighting matrix. The states included in the optimization vector are

$$\mathbf{z} = \begin{bmatrix} p_N & p_E & h & u \end{bmatrix}^\intercal. \tag{3.6}$$

The function $\mathbf{h}$ is where the distance between the reference signal and the UAV states is calculated. For the the north-east position of the camera centre point is compared to the observation path, while the height h and speed u is compared to a constant reference signal h_d and u_d respectively:

$$\mathbf{h} = \begin{bmatrix} p_N - p_{Nd} \\ p_E - p_{Ed} \\ h - h_d \\ u - u_d \end{bmatrix}. \tag{3.7}$$

In order to reduce the control effort for the optimization problem the rate of change of the control inputs $d\mathbf{u}$ will be minimized. Since all the control rates is to be compared to zero no function is needed. The matrix $\mathbf{R}$ is the weighting matrix. The vector u contains of the four control rates:

$$\mathbf{u} = \begin{bmatrix} d\delta_e & d\delta_a & d\delta_r & d\delta_t \end{bmatrix}^\intercal. \tag{3.8}$$

3.4.2 Prediction Model

The linear decoupled 12 DOF UAV model presented by Beard & McLain [13] will be implemented. This model is associated with the following states and control inputs:

$$\mathbf{x} = \begin{bmatrix} p_N & p_E & h & u & v & w & \phi & \theta & \psi & p & q & r \end{bmatrix}^T \tag{3.9a}$$

$$\mathbf{u} = \begin{bmatrix} \delta_e & \delta_a & \delta_r & \delta_t \end{bmatrix}^T. \tag{3.9b}$$

The prediction model relates to the equality constraints of equation 3.1 in the form of differential equations. Based on the control inputs and current states, $\dot{\mathbf{x}}$ is calculated by the differential equation. The attitude angles will be expressed in Euler angles. Even though quaternions offer more efficient computations and no gimbal lock [13], this optimization will be run on an offboard computer/offline so that computation capacity is not a big issue and the UAV is not going to undergo any extreme maneuvers so that a gimbal lock should never occur.

3.4.3 Control Law

The only physical constraints in this optimization problem is constraints on the control inputs, as shown in equation 3.10. This inequality constraint ensures that the control surfaces of the UAV simulated in the optimization do not excede what the UAV is physically capable of.

$$\mathbf{u}^{low} \leq \mathbf{u} \leq \mathbf{u}^{high} \tag{3.10}$$

Chapter 4

Optimization Implementation

4.1 ACADO toolkit

Chapter 5

MPC Implementation

Appendices

Appendix A

ACADO Code

Appendix B

MPC Code

Bibliography

[1] E. Skjong, S. A. Nundal, F. S. Leira, and T. A. Johansen. 2015 international conference on unmanned aircraft systems (ICUAS). In *Autonomous Search and Tracking of Objects Using Model Predictive Control of Unmanned Aerial Vehicle and Gimbal: Hardware-in-the-loop Simulation of Payload and Avionics*, Denver, Colorado, USA, June 2015. IEEE.

[2] J. Egbert and R. W. Beard. Proceedings of the 2007 American control conference. In *Low Altitude Road Following Constraints Using Strap-Down EO Cameras on Miniature Air Vehicles*, New York City, USA, July 2007. IEEE.

[3] Thomas M. Fisher. Rudder augmented trajectory correction for unmanned aerial vehicles to decrease lateral image errors of fixed camera payloads. *All Graduate Theses and Dissertations*, 2016.

[4] S. Mills, J. J. Ford, and L. Mejias. Vision based control for fixed wing UAVs inspecting locally linear infrastructure using skid-to-turn maneuvers. *Journal of Intelligent and Robotic Systems*, 61(1):29–42, 2011.

[5] M. Ahsan, H. Rafique, and Z. Abbas. Multitopic conference (INMIC). In *Heading Control of a Fixed Wing UAV Using Alternate Control Surfaces*. IEEE, December 2012.

[6] T. Inanc, K. Misovec, and R. M. Murray. 43rd IEEE conference on decision and control. In *Nonlinear Trajectory Generation for Unmanned Air Vehicles with Multiple Radars*, Atlantis, Paradise Island, Bhamas, December 2004. IEEE.

[7] Anders la Cour-Harbo and Morten Bisgaard. *State-Control Trajectory Generation for Helicopter Slung Load System using Optimal Control*. American Institute of Aeronautics and Astronautics Meeting Papers on Disc. 2009.

[8] Stephen P. Jackson. Controlling small fixed wing UAVs to optimize image quality from on-board cameras. *ProQuest Dissertations and Theses*, 2011.

[9] Randall B. Smith. *Introduction to Hyperspectral Imaging*. MicroImages, Inc., 2012.

[10] R. Nsi, E. Honkavaara, P. Lyytikinen-Saarenmaa, M. Blomqvist, P. Litkey, T. Hakala, N. Viljanen, T. Kantola, T. Tanhuanp, and M. Holopainen. Using

UAV-based photogrammetry and hyperspectral imaging for mapping bark beetle damage at tree-level. *Remote Sensing*, 7(15467-15493), 2015.

[11] P. J. Zarco-Tejada, V. Gonzlez-Dugo, and J. A. J. Berni. Fluorescence, temperature and narrow-band indices acquired from a UAV platform for water stress detection using a micro-hyperspectral imager and a thermal camera. *Remote Sensing of Environment*, 117(322-337), 2012.

[12] J. Suomalainen, N. Anders, S. Iqbal, G. Roerink, J. Franke, P. Wenting, D. Hnniger, H. Bartholomeus, R. Becker, and L. Kooistra. A lightweight hyperspectral mapping system and photogrammetric processing chain for unmanned aerial vehicles. *Remote Sensing*, 6(11013-11030), 2014.

[13] Randal W. Beard and Timothy W. McLain. *Small Unmanned Aircraft: Theory and Practice*. Princeton University Press, Princeton, NJ, USA, 2012.

[14] E. F. Camacho and Bordons C. *Model Predictive Control*. Springer London, 1999.

[15] J. Nocedal and S. Wright. *Numerical Optimization*. Springer Series in Operations Research and Financial Engineering. Springer New York, 2006.

[16] J. B. Rawlings and D. Q. Mayne. *Model Predictive Control: Theory and Design*. Nob Hill Publishing, Madison, Wisconsin, 2015.

[17] W. H Kwon and S. H. Han. *Receding Horizon Control: Model Predictive Control for State Models*. Advanced Textbooks in Control and Signal Processing. Springer London, 2005.